Rock and Soil Mechanics

Volume 41 | Issue 2 Article 5

9-27-2020

Study on anisotropic permeability model for mixed kaolin-montmori- llonite clays

Jie XU
Engineering Research Center of Urban Underground Development of Zhejiang Province, Hangzhou, 310058, China

Jian ZHOU
Engineering Research Center of Urban Underground Development of Zhejiang Province, Hangzhou, 310058, China

Ling-hui LUO
Engineering Research Center of Urban Underground Development of Zhejiang Province, Hangzhou, 310058, China

Liang-gui YU
Engineering Research Center of Urban Underground Development of Zhejiang Province, Hangzhou, 310058, China

Custom Citation

XU Jie, ZHOU Jian, LUO Ling-hui, YU Liang-gui, . Study on anisotropic permeability model for mixed kaolin-montmori- llonite clays[J]. Rock and Soil Mechanics, 2020, 41(2): 469-476.

Rock and Soil Mechanics 2020 41(2): 469–476 ISSN 1000–7598
https: //doi.org/10.16285/j.rsm.2019.5056 rocksoilmech.researchcommons.org/journal

Study on anisotropic permeability model for mixed kaolin-montmorillonite clays

XU Jie[1, 2], ZHOU Jian[1, 2], LUO Ling-hui[1, 2], YU Liang-gui[1, 2]

1. Research Center of Coastal and Urban Geotechnical Engineering, Zhejiang University, Hangzhou, 310058, China
2. Engineering Research Center of Urban Underground Development of Zhejiang Province, Hangzhou, 310058, China

Abstract: A perfect anisotropic permeability model is helpful to guide the drainage and grouting scheme of underground buildings during construction and operation period. To study permeability anisotropy model, mixed kaolinite-montmorillonite clays were used in a series of permeation experiments by triaxial permeameter, and the development of anisotropic permeability model was attempted from both macroscopic and microscopic perspectives. The results show that: as the amount of bentonite increases, the small pores increase, but the large pores decrease; as the consolidation stress increases, all pores decrease, and the maximum pore size decreases. Macroscopically there is no correlation between the void ratio considering the liquid limit void ratio and the permeability anisotropic ratio, which indicates that the void ratio e and liquid limit void ratio e_L are not the key parameter determining the permeability anisotropy ratio. The permeability anisotropy model expressed by microscopic parameters indicates that it is not only feasible to explore the permeability anisotropy model from the microscopic point, but also to reveal the essence of permeability anisotropy. In all microscopic models, the permeability anisotropy model expressed by pore indexes $D_{50} - D_{70}$ is well correlated, which can reflect changes in larger pores.

Keywords: mixed clay; permeability anisotropy model; macroscopic parameter; microscopic parameter; pore index

1 Introduction

Soft clay has permeability anisotropy due to sedimentary environment and loading[1]. The horizontal permeability coefficient k_h and vertical permeability coefficient k_v of the soil can be measured, and the ratio of the two values is defined as the permeability anisotropy, which can reflect the anisotropy in permeability. A perfect permeability anisotropy model is helpful to guide the selection of engineering schemes during construction and operation of underground structures[2]. It is thus necessary to carry out a systematic study on the permeability anisotropy model for construction of underground structures in clay formation.

At present, the research on the permeability model is relatively comprehensive. Most scholars study the permeability model from the aspects of void ratio, limit moisture content, and micro parameters. The summary of the existing research results is shown in Table 1. The earliest permeability model was proposed based on the void ratio, and established for sand by Kozeny[3], after that Taylor[4] established a semi-logarithmic permeability model for soft clay. Mesri[5] established a double-logarithmic permeability model expressed by void ratio for soft clay, which enriched the expression form of the permeability model. Yang et al. [6] added a new variable (clay content) to the semi-logarithmic permeability model, while this model was extremely complicated.

Clay characteristics have a close relationship with the limit moisture content. Chapuis[7] argued that the specific surface area of the soil should be considered when studying the permeability model, and there is a certain relationship between the specific surface area and the limit moisture content of the soil. Thus a good permeability model should also consider the limit moisture content. Nishida et al.[8] analyzed the consolidation settlement data of the soil and obtained the permeability model expressed by plasticity index. Sivappulaiah et al.[9] conducted the seepage test using a mixture of sand and bentonite, and obtained the permeability model expressed by liquid limit water content. With the following research of the permeability model, the liquid limit void ratio e_L was gradually used to replace the limit water content. Nagaraj et al.[10] proposed a comprehensive permeability model $e / e_L = A + B\lg k$. For different soils, the parameters A and B have different values [10–11]. In addition to the void ratio and the limit moisture content, there are also some permeability models which are expressed by effective stress, strain, burying depth and compaction. These models are derived from the void ratio as an intermediate variable. Therefore, these models are essentially the permeability model expressed by void ratio.

Received: 10 January 2019 Revised: 29 April 2019
This work was supported by the National Key Research and Development Program of China (2016YFC0800203) and the National Natural Science Foundation of China (51338009).
First author: XU Jie, male, born in 1993, Postgraduate, majoring in the permeability of soft clay. E-mail: 981730290@qq.com
Corresponding author: ZHOU Jian, female, born in 1970, Professor, PhD supervisor, Research interests: soft clay mechanics, soft soil foundation treatment and unsaturated soil constitutive model. E-mail: zjelim@zju.edu.cn

The above-mentioned permeability models are all from macro-scale perspective, and some scholars have tried to explore the permeability model from micro-scale perspective. Carcia et al.[12] tried to establish a relationship between permeability coefficients and Pore-Size Parameters (PSP), which can be calculated by using capillary water model, head radius model and probability model. Tanaka et al.[13] pointed out that under different pressures, a linear relationship between the permeability coefficient and the pore coefficient r_{50} can be established, and this linear relationship was then validated by Ninjgarav et al[14]. Rao[15] established a functional relationship between the permeability coefficient and the pore fractal dimension. These permeability models are all established from micro-scale perspective.

At present, there lacks of systematical research on the permeability anisotropy model. Witt et al.[16] used the square of the tortuosity of the seepage channel (seepage path length / geometric length) to express the permeability anisotropy. Chapuis et al.[17] carried out seepage tests on sand and cohesive soil, and found the relationship between the permeability anisotropy and the void ratio is in exponential form, the smaller the void ratio, the greater the permeability anisotropy ratio, an exponential permeability anisotropy model was thus proposed. Adams et al.[18] proposed a linear permeability anisotropy model expressed by the void ratio based on the study of Boston blue clay, the proposed model failed to reflect the characteristics of the soil microstructure because the void ratio is a macro parameter of the soil. The micro structure of the soil has a great influence on the permeability coefficient, because the pore distribution is irregular and non-linear, and affects the flow of water inside the soil. Therefore, the permeability anisotropy model that only considers the macro-scale parameters cannot reveal the essence of permeability anisotropy. It can be seen that the existing permeability anisotropy models are not comprehensive due to lack of the essence of the permeability anisotropy, and the permeability anisotropy ratio could not be accurately calculated, their applicability is thus very limited.

Although the problem of permeability anisotropy has attracted attention, the research on permeability anisotropy model is very rare. It can be seen that pore characteristics, liquid properties and mineral types can affect the permeability of clay, therefore the kaolin-montmorillonite mixed clay is studied in this work, and the triaxial seepage samples are cut horizontally and vertically to conduct the seepage test to obtain the permeability coefficient, and then the permeability anisotropy of the soil is calculated. In addition, systematic research on the micro structure of the mixed clays is performed in order to further explore the influence factors of both the permeability anisotropy and the permeability anisotropy models.

Table 1 Summary of model research status

Model	Research perspective	Influence factors	Typical model	The meaning of parameters	References
Permeability model	Macro	Void ratio	$\lg e = A + B\lg k$	k is the permeability coefficient; e is the void ratio; A and B are model parameters.	Kozeny [3], Taylor [4], Mesri [5]
	Macro	Limit moisture content	$e / e_{\mathrm{L}} = A + B\lg k$	e_{L} is the liquid limit void ratio.	Nagaraj et al.[10], Achari et al.[11]
	Macro	Other	$k = k_0 \mathrm{e}^{-ap}$	k_0 is the initial void ratio; p is the consolidation pressure; a is the parameter.	Loius [19], Potts et al.[20], Wang et al.[21]
	Micro	Pore parameter	$k = 3.64\times10^{-12}\mathrm{PSP}^{7.58}$	PSP is the pore parameter.	Tanaka et al.[13], Ninjgarav et al.[14], Kong [22], Rao[15]
Permeability anisotropy model	Macro	Void ratio	$r_{\mathrm{k}} = -4.63e + 3.54$ $(0.36 < e < 0.5)$	r_{k} is the permeability anisotropy ratio.	Chapuis et al. [17], Adams et al. [18]
	Micro	The tortuosity of the seepage channel	$r_{\mathrm{k}} = \frac{k_{\mathrm{h}}}{k_{\mathrm{v}}} = \left(\frac{T_{\mathrm{v}}}{T_{\mathrm{h}}}\right)^2$	T_{h} and T_{v} are the tortuosity of seepage channel for horizontal and vertical sections respectively.	Witt et al.[16]

2 Test process and test plan

2.1 Sample preparation

Kaolin has been widely used in the research of geotechnical engineering as an artificial clay due to its standardization and relatively high permeability[23]. In laboratory test, kaolin is often mixed with sand, silt or other chemical materials to simulate the marine clay. On the other hand, as a highly compressible clay, bentonite has a higher limit moisture content than kaolin. Because the limit moisture content is a key factor affecting the permeability coefficient, consolidation pressure and liquid properties have a greater influence on the permeability coefficient of bentonite than that of kaolin clay [24]. Therefore, the kaolin-montmorillonite mixed clay is studied in

the present work to reveal the essence of permeability anisotropy of clay.

The kaolin used in this test is Malaysian kaolin, and bentonite is from Chifeng city. The corresponding kaolinite and montmorillonite mineral content are both above 95%. Kaolin and bentonite are mixed according to the mineral proportion requirements, and the mixed mineral is fully stirred with ultrapure water according to the mass ratio of mineral to water (1: 2). After that the slurry is poured into a 180 mm×650 mm (diameter × height) plexiglass barrel and allowed to stand for 24 h. Apply pressure to the plexiglass barrel under the consolidation instrument until the pressure is reached to 95 kPa, and divide this stage into three phases and each phase lasts 48 h. After the loading stage is completed, the moisture content of the remolded clay is between 58% and 60%, and the remolded clay is relatively uniform. In horizontal and vertical directions, cut the prepared remolded clay into a triaxial sample with 140 mm in height and 70 mm in diameter. The sample is then installed in the GDS triaxial permeameter to perform the seepage test. The specific sample preparation process to study the permeability characteristics of kaolin could refer to Yu[23].

2.2 Test procedure

The prepared triaxial sample was installed on the GDS triaxial permeameter, and the seepage test process was divided into 3 steps, i.e. saturation, consolidation, and seepage. The specific test process is described as follows:

(1) Saturation stage: The sample was saturated at a backpressure of 100 kPa. To ensure the Skempton's pore pressure parameter B is higher than 0.98.

(2)Consolidation stage: The sample was consolidated under an effective consolidation pressure of 100 kPa, this stage lasted until the volume of water squeezed out from the specimen less than 100 mm^3 per hour.

(3)Seepage stage: The back pressure at the bottom and top of the specimen were designed as $100 + \Delta u / 2$ and (kPa) and $100–\Delta u / 2$ (kPa)the back pressure, respectively, where Δu is the pore water pressure difference between the bottom and top of the specimen under the design hydraulic gradient. The hydraulic gradient was set to 10 according to the selection of the hydraulic gradient proposed by Yu [23].

It should be noted that when studying the effects of liquid properties, it is necessary to add an isolator to prevent the solution from corroding the controller.

2.3 Micro-scale test

According to the micro-scale test method of Cao [25], the sample after the seepage test was cut into a sample with size of 20 mm×5 mm×5 mm (height × length × width) along the seepage direction for the micro-scale test. The FEI Nova NanoSEM 450 ultra-high-resolution scanning electron microscope of Zhejiang University School of Medicine was used for the electron microscopy scanning test. Under the electron microscope, the sample was magnified 16,000 times and high-quality scanning images were taken. Quantitative analysis of the scanning images was performed using the Particle and Crack Analysis System (PCAS) of Nanjing University. The microstructures of S2VP1 and S2HP1 are shown in Fig.1.

Figures 1 (a) and (b) are the scanning images, and (c) and (d) are processed images by PCAS. White areas represent pores and black areas represent clay particles. The images used in this paper are all 1 536× 1 103 pixels. The actual size of images is 25.9 μm×18.6 μm, and the image resolution is 59.3 pixels/μm.

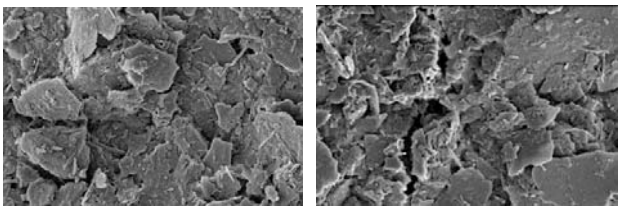

(a) The scanning image (vertical) (b) The scanning image (horizontal)

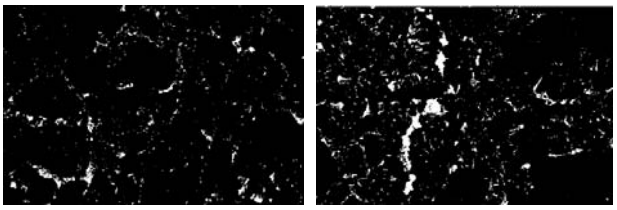

(c) The processed image (vertical) (d) The processed image (horizontal)

Fig.1 Micro structures of B20K80V and B20K80H

2.4 Test plan

In order to explore a reasonable and complete permeability anisotropy model, a reasonable test scheme, which should be able to study the effects of pore characteristics, liquid properties, and clay mineral types on permeability anisotropy, is necessary. The final test plan is shown in Table 2.

Because the mineral content of montmorillonite in marine clay and underground clay is generally below 25% [26], the content of bentonite (B) is set to 5%, 10%, and 20%, the corresponding mixed clay samples are named as B5K95, B10K90, and B20K80, respectively, where the number after the letter represents the content. At the same time, pure kaolin (K) is used as the control group test, and c stands for molar concentration.

Table 2 Experimental program

Number	Number	Liquid properties	Concentration / (mol/L)	Consolidation pressure / kPa
S1HP1	S1VP1	Pure water	—	100
S1HP2	S1VP2	Pure water	—	200
S1HP3	S1VP3	Pure water	—	300
S2HP1	S2VP1	Pure water	—	100
S2HP2	S2VP2	Pure water	—	200
S2HP3	S2VP3	Pure water	—	300
S3HP1	S3VP1	NaCl solution	0.1	100
S3HP2	S3VP2	NaCl solution	0.1	200
S3HP3	S3VP3	NaCl solution	0.1	300
S4HP1	S4VP1	NaCl solution	0.1	100
S4HP2	S4VP2	NaCl solution	0.1	200
S4HP3	S4VP3	NaCl solution	0.1	300
S5HP1	S5VP1	Pure water	—	100
S6HP1	S6VP1	Pure water	—	100

Note: S1, S2, S3, S4, S5, and S6 represent B5K95, B20K80, B5K95c0.1,B20K80c0.1,K, and B10K90 ,respectively. H and V represent horizontal and vertical directions, respectively. P represents consolidation pressure, and P1 , P2, and P3 indicate that the consolidation pressures are 100, 200, and 300 kPa, respectively.

3 Pore gradation curve

The pore distribution is irregular and non-linear, and the mercury intrusion test provides an effective solution to study the relationship between the pore distribution and permeability coefficient. As early as 1990, Lapierre et al.[27] obtained the relationship between the pore distribution and permeability coefficient of the undisturbed soil and the remolded soil according to the mercury intrusion test, and further proposed three classic permeability models. Other scholars consequently used the mercury intrusion test to study the consolidation and permeability characteristics of soils[10,14,23,28]. However, the mercury intrusion test is based on many assumptions, such as the cylindrical equivalent of the pore and no deformation in the soil skeleton under external pressure.Considering that the microstructure difference between horizontal and vertical directions of the same sample is studied in this work, while the pore parameters obtained from the mercury intrusion test are non-directional, which makes the mercury intrusion test unable to distinguish the micro structure difference between horizontal and vertical directions of the same sample. Therefore, the mercury intrusion test fails to study permeability anisotropy.

The scanning electron microscope (SEM) method can solve the problem of failure to distinguish the pore characteristics difference between horizontal and vertical microstructures of the same sample in the mercury intrusion test. By processing the SEM images, it is possible to study the differences in the microstructure of the same sample in different directions, which brings new insights into the study of permeability anisotropy. This paper will use the SEM method to analyze the microstructure of the same sample in different directions, and try to find a more applicable permeability anisotropy model from the micro-scale perspective.

The pore gradation curve is an important curve to characterize the continuity of pores in the soil. In this paper, the pore gradation curve is used to study the permeability anisotropy of the soil under different working conditions. Through the micro-scale test method introduced in Section 2.3, the pore data obtained by the PCAS can be drawn into the pore gradation curve.

3.1 Mineral content analysis

Taking the pore gradation curves of three vertical samples (i.e., pure kaolin K, mixed clay B5K95, mixed clay B20K80) under the effective consolidation pressure of 100 kPa as examples, the pore gradation curves of three samples are shown in Fig.2, the horizontal axis is the pore diameter and the vertical axis is the ratio of pore area smaller than a certain size to total pore area.

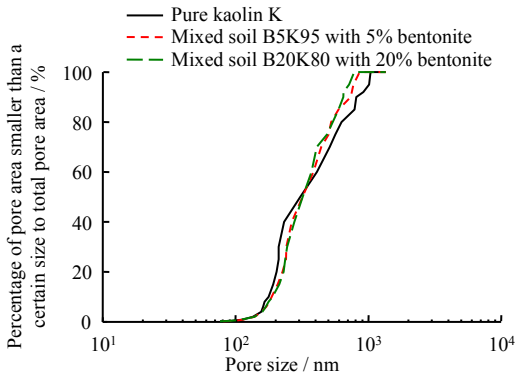

Fig.2 Pore gradation curve of mixed clay in different bentonite fractions (100 kPa)

It can be seen from Fig.2 that with increasing of the bentonite content, the pore less than 200 nm in the mixed clay does not change significantly, and the pore between 200 and 400 nm increases, while the pore larger than 400 nm decreases. It should be noted that the maximum pore diameter in the mixed clay decreases from 1 040 to 780 nm. In general, with increasing of the bentonite content, the small pore in the mixed clay remains unchanged, and the medium pore increases, and the large pore decreases, and the maximum pore size significantly becomes smaller.

In fact, the specific surface area of montmorillonite mineral clay is obviously higher than that of kaolinite mineral clay, and the montmorillonite mineral clay has a strong water-swelling ability, the limit moisture content of bentonite is thus higher than that of kaolin [29–30]. At the same time, bentonite is rich in

small pores, while pore size of kaolin is relatively larger [30], the permeability coefficient of bentonite is thus much smaller than that of kaolin. Therefore, when bentonite is added into kaolin, pores of the mixed clay will gradually become smaller, this results in the medium pore increases and the large pore decreases with increase of the bentonite content.

3.2 Consolidation pressure analysis

Similarly, the vertical samples of B5K95 under the effective consolidation pressures of 100 kPa and 300 kPa are used in order to study the variation of the pore gradation curve under different pressures. The pore gradation curve is shown in Fig. 3.

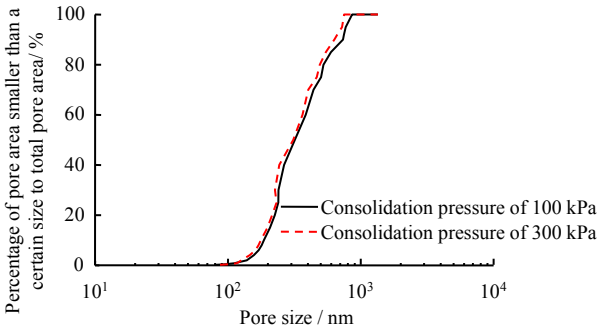

Fig.3 Pore gradation curves of mixed clay at different consolidation pressures (B5K95)

It can be known from Fig.3 that the pore gradation curve moves to the left and pore diameter becomes smaller and the maximum pore diameter becomes smaller with increasing of the consolidation pressure. With increase of the consolidation pressure, the pore less than 200 nm does not change significantly, the pore larger than 200 nm decreases significantly. Previous studies have shown that [13–14, 27, 31], the large pores in the soil will be compressed into small pores under pressure, consequently makes the large pores decrease. This phenomenon is confirmed by the test results in this work.

Ninjgarav et al.[14] obtained the pore gradation curves of the soil with different burial depths in the Luodong River Plain by the mercury intrusion test. The test results indicated that the large pore obviously decreases and the proportion of large pore decreases with increasing of the consolidation pressure. Some other scholars also obtained similar conclusions from the analysis of pore gradation curves of clays in different regions [13,22,27].

The pore gradation curve of the soil at 18 m depth under different pressures obtained by Ninjgarav et al.[14] is plotted in Fig.4. By comparing Fig.3 and Fig.4, it is found that the test results obtained in this paper is similar to the pore gradation curves of the 80 kPa and 140 kPa in Fig.4, which corresponds to the pore size range from 0.1 to 1 μm by Ninjgarav et al. [14]. In other words, with increasing of the consolidation pressure, the pore gradation curve moves to the left, pores become significantly smaller, the large pores decrease, and the maximum pore diameter decreases.

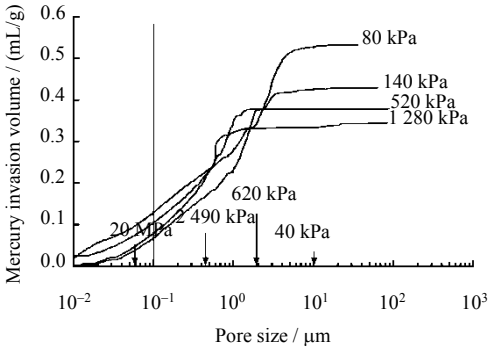

Fig.4 Pore gradation curves of mixed clay at different applied stresses [14]

4 Permeability anisotropy model

4.1 Macro parameter study

From Table 1, it can be seen that the existing permeability anisotropy model is expressed by void ratio and tortuosity of pore channels, and the permeability anisotropy model expressed by void ratio is proposed for Boston blue clay. For soils with different mineral components, the applicability of the existing permeability anisotropy model needs further research, and the permeability anisotropy model on the basis of the existing permeability models is investigated in this paper. Among them, the highly recognized permeability model considers both the void ratio and the limit moisture content of the soil, and is shown as

$$e / e_{\mathrm{L}} = A + B \lg k \tag{1}$$

The void ratio is a three-dimensional volume parameter, so that the void ratio and the liquid limit void ratio of the same sample is the same horizontally and vertically, therefore the horizontal and vertical semi-logarithmic permeability models are written as

$$e / e_{\mathrm{L}} = A_{\mathrm{h}} + B_{\mathrm{h}} \lg k_{\mathrm{h}} \tag{2}$$

$$e / e_{\mathrm{L}} = A_{\mathrm{v}} + B_{\mathrm{v}} \lg k_{\mathrm{v}} \tag{3}$$

where A_{h}, A_{v}, B_{h}, and B_{v} are the model parameters in the horizontal and vertical permeability models, respectively.

According to the following definition of permeability anisotropy:

$$r_{\mathrm{k}} = \frac{k_{\mathrm{h}}}{k_{\mathrm{v}}} \tag{4}$$

Substituting Eqs. (2) and (3) into Eq. (4):

$$r_k = \exp\left(\frac{e/e_L - A_h}{B_h} - \frac{e/e_L - A_v}{B_v}\right) \quad (5)$$

Sorting Eq. (5) to get:

$$\frac{e}{e_L} = \frac{A_h B_v - A_v B_h}{B_v - B_h} + \frac{B_v B_h}{B_v - B_h}\lg r_k \quad (6)$$

That is

$$\frac{e}{e_L} = C + D\lg r_k \quad (7)$$

where parameter, $C = \frac{A_h B_v - A_v B_h}{B_v - B_h}$,parameter, $D = \frac{B_v B_h}{B_v - B_h}$.

It can be seen that the relationship between the permeability anisotropy γ_k and the macro-scale parameter e/e_L is semi-logarithmic. Based on this, the void ratio, liquid limit void ratio and permeability anisotropy of the sample were measured in this paper, and the test results are shown in Table 3.

Table 3 Macro-scopic test results

Number	k_v / (10^{-7} cm/s)	k_h / (10^{-7}cm/s)	$r_k = \frac{k_h}{k_v}$	Void ratio e	liquid limit void ratio e_L	e / e_L
S1P1	8.35	10.39	1.244	1.43	1.82	0.785
S1P2	5.81	8.01	1.379	1.33	1.82	0.733
S1P3	4.41	6.19	1.400	1.26	1.82	0.694
S2P1	5.19	6.46	1.245	1.39	2.18	0.637
S2P2	3.04	4.17	1.372	1.24	2.18	0.569
S2P3	1.73	2.41	1.393	1.14	2.18	0.523
S3P1	7.65	9.56	1.250	1.42	1.84	0.772
S3P2	5.11	7.04	1.378	1.30	1.84	0.706
S3P3	4.22	5.86	1.389	1.22	1.84	0.664
S4P1	5.47	6.78	1.239	1.31	2.24	0.584
S4P2	3.4	4.54	1.335	1.17	2.24	0.520
S4P3	2.14	2.87	1.341	1.06	2.24	0.474
S5P1	15.28	21.19	1.387	1.58	1.86	0.850
S6P1	7.15	8.97	1.255	1.40	1.91	0.731

Based on the test results and the permeability anisotropy model derived from Eq. (7), a fitting relationship between the permeability anisotropy and the macro parameters (void ratio and liquid limit void ratio) is established and shown in Fig.5. The permeability anisotropy model expressed by the macroscopic parameter is not effective and its correlation coefficient is only 0.065. It shows that the two macro parameters of void ratio and liquid-limiting void ratio cannot reflect the feature of permeability anisotropy. Based on this phenomenon and previous studies [6, 13–16, 18, 29], the permeability anisotropy model from the micro-scale perspective is attempted in this work.

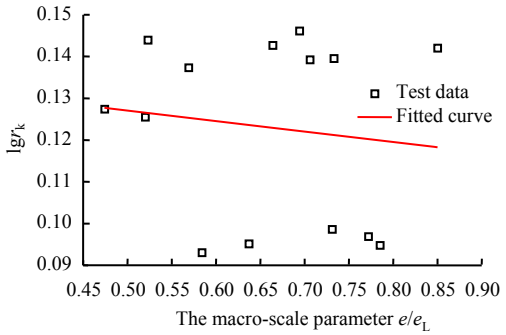

Fig.5 Relationship between permeability anisotropy ratio r_k and macroscopic parameters e/e_L

4.2 Micro-scale permeability anisotropy model

4.2.1 Definition of micro-scale parameters

Tanaka et al.[13] studied the permeability coefficients and the corresponding pore gradation curves of soft clays in different regions, and found that the relationship between the permeability coefficient and the pore coefficient r_{50}^2 is linear(where r_{50} denotes the pore diameter corresponding to 50% cumulative pore volume percentage of pore less than this pore diameter versus the total pore volume on the pore gradation curve, similarly hereinafter). Rao[15] conducted seepage tests on remolded clays with different dry densities in Wuhan Hanjie, r_{30}^2, r_{40}^2, r_{50}^2, r_{60}^2, r_{70}^2 are used to study the permeability model, and the predicted value of the permeability model expressed by r_{60}^2 is very close to the actual value. It can be seen that the permeability model established from the micro-scale perspective is gradually recognized, while the permeability anisotropy model from the micro-scale perspective is very rare. The pore coefficient can directly reflect the pore size and content, and the permeability model expressed by the pore coefficient can reflect the continuity and distribution of pores in the soil. From this perspective, it is feasible to establish the permeability anisotropy model expressed by the pore coefficient.

With reference to the research method of Rao[15], the corresponding pore size coefficient is selected as the research object based on the pore gradation curve in this work. The pore size coefficients in the horizontal and vertical directions of the same sample are respectively obtained, and the ratio of the two cases is then squared as the aperture index. Taking the calculation of the aperture index D_{70} as an example, and the formula is described as follows:

$$D_{70} = \frac{r_{h70}^2}{r_{v70}^2} \quad (8)$$

where r_{h70} and r_{v70} are the pore diameters corresponding to 70% cumulative pore area percentage of pore less than this

pore diameter versus the total pore area on the horizontal and vertical seepage profiles of the pore gradation curve. In the same way, the aperture indexes D_{30}, D_{40}, D_{50}, and D_{60} can be obtained.

4.2.2 Micro-scale permeability anisotropy model

Most of the existing permeability models are semi-logarithmic, the permeability anisotropy model based on the semi-logarithmic relationship is thus adopted in this work, and the semi-logarithmic permeability anisotropy model expressed by the aperture index (D_{30}, D_{40}, D_{50}, D_{60}, D_{70}) is established. The test results are shown in Table 4.

Table 4 Microscopic model test results

Number	r_k	$\lg r_k$	D_{30}	D_{40}	D_{50}	D_{60}	D_{70}
S1P1	1.244	0.095	1.156	1.42	1.163	1.199	1.347
S1P3	1.400	0.146	1.467	1.532	1.617	2.197	1.808
S2P1	1.245	0.095	1.203	1.306	1.079	1.134	1.311
S3P1	1.250	0.097	1.158	1.376	1.016	1.306	1.332
S4P1	1.239	0.093	1.151	1.392	1.101	1.162	1.318
S5P1	1.387	0.142	1.118	1.432	1.601	1.597	2.141
S6P1	1.255	0.099	1.168	1.354	1.139	1.375	1.368

The permeability anisotropy ratio and the aperture index in Table 4 are fitted to obtain the corresponding micro-scale permeability anisotropy model, and the correlation coefficients of each model are summarized in Table 5 to compare their difference.

Table 5 Microscopic permeability anisotropy model

Number	Independent variable (x)	$\lg r_k$ (y)	Correlation coefficient
1	D_{30}	y=0.153x–0.075	0.728
2	D_{40}	y=0.205x–0.183	0.776
3	D_{50}	y=0.092x–0.005	0.950
4	D_{60}	y=0.051x+0.033	0.983
5	D_{70}	y=0.108x–0.048	0.995

In Table 5, the correlation of the permeability anisotropy model is better with the aperture index larger. In general, the correlation of obtained permeability anisotropy models is obviously high when the aperture index is between D_{50} and D_{70}. If D_{70} is selected as the independent variable to establish the permeability anisotropy model, the correlation coefficient of the model is close to 1. Therefore, the aperture index D_{70} can be considered as the determining parameter of the permeability anisotropy. The permeability anisotropy model expressed by the aperture index D_{70} is shown in Fig. 6.

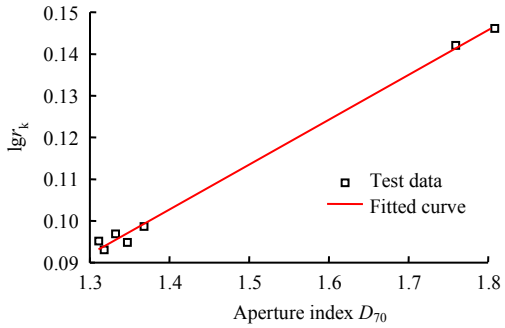

Fig.6 Microscopic permeability anisotropy model (Taking D_{70} as the example)

According to the analysis in Section 3, it can be seen that the effect of the consolidation pressure and the bentonite content on the pore gradation curve is mainly concentrated on pores larger than 200 nm. When external factors change, the change of small pores in soil is not as large as that of large pores, and the permeability anisotropy is closely related to the change of large pores, and the aperture indexes D_{50}–D_{70} that can reflect the change of large pores are the determining parameter that affects the permeability anisotropy. Therefore, the permeability anisotropy model expressed by the aperture indexes D_{50}–D_{70} is better.

The permeability anisotropy model that can be suitable for kaolin-montmorillonite mixed clays and is given as

$$\lg r_k = 0.108 D_{70} - 0.048 \quad (9)$$

5 Conclusions

The permeability anisotropy characteristics of kaolin-montmorillonite mixed clays from both macro-scale and micro-scale perspectives were studied and the following conclusions could be derived:

(1) With increasing of the bentonite content, the pore between 200 and 400 nm in the mixed clay increases, and the pore larger than 400 nm decreases. With increasing of the consolidation pressure, the pore larger than 200 nm decreases, and the maximum pore diameter decreases.

(2) There is no obvious relationship between the two macro-scale parameters (void ratio and liquid limit void ratio) and the permeability anisotropy, which indicates macro-scale parameters are not the determining parameter of permeability anisotropy.

(3) The permeability anisotropy model expressed by micro-scale parameters shows good agreement. It is not only feasible to study the permeability anisotropy from the micro-scale perspective, but can also reveal the essence of permeability anisotropy. The aperture indexes of D_{50}–D_{70},

which can reflect the change of large pores, are the determining parameter of the permeability anisotropy, and the micro-scale permeability anisotropy model expressed by the aperture indexes of D_{50}–D_{70} is better.

References

[1] TAVENAS F, JEAN P, LEBLOND P, et al. The permeability of natural soft clays. part II: permeability characte[J]. Canadian Geotechnical Journal, 1983, 20(4): 645–660.

[2] KE Han, WU Xiao-wen, ZHANG Jun, et al. Modeling saturated permeability of municipal solid waste based on compression change of its preferential flow and anisotropy[J]. Chinese Journal of Geotechnical Engineering, 2016, 38(11): 1957–1964.

[3] KOZENY J. Über kapillare Leitung des Wassers im Boden[J]. Akad. Wiss. Wien, 1927, 136: 271–306.

[4] TAYLOR D W. Fundamentals of soil mechanics[M]. New York: John Wiley & Sons Inc., 1948.

[5] MESRI G. Mechanisms controlling the permeability of clays[J]. Clays and Clay Minerals, 1971, 19(3): 151– 158.

[6] YANG Y, APLIN A C. Permeability and petrophysical properties of 30 natural mudstones[J]. Journal of Geophysical Research, 2007, 112: B03206.

[7] CHAPUIS R P. Predicting the saturated hydraulic conductivity of soils: a review[J]. Bulletin of Engineering Geology and the Environment, 2012, 71(3): 401–434.

[8] NISHIDA Y, NAKAGAWA S. Water permeability and plastic index of soils[C]//Proceedings of IASH-UNESCO Symposium. Tokyo city: Land Subsidence, 1969: 573–578.

[9] SIVAPPULAIAH P V, SRIDHARAN A, STALIN V K. Hydraulic conductivity of bentonitesand mixtures[J]. Canadian Geotechnical Journal, 2000, 37(2): 712–722.

[10] NAGARAJ T S, PANDIAN N S, RAJU P S R N. Stress-state-permeability relations for overconsolidated clays[J]. Géotechnique, 1994, 44(2): 349–352.

[11] ACHARI G, JOSHI R C. A reexamination of the permeability index of clays: discussion[J]. Canadian Geotechnical Journal, 1994, 31(1): 140–141.

[12] GARCIA B I, LOVELL C W, ALTSCHAEFFLA G. Pore distribution and permeability of silty clays[J]. Journal of the Geotechnical Engineering Division, 1979, 105: 839–856.

[13] TANAKA H, SHIWAKOTI D R, OMUKAI N, et al. Pore size distribution of clayey soils measured by mercury intrusion porosimetry and its relation to hydraulic conductivity[J]. Soils and Foundations, 2003, 43(6): 63–73.

[14] NINJGARAV Enebish, CHUNG Sung-gyo, JANG Woo-young. Pore size distribution of pusan clay measured by mercury intrusion porosimetry[J]. Geotechnical Engineering, 2007, 11(3): 133–139.

[15] RAO Tian-kuan. Different clayey soil compaction degree study on the relationship between the microscopic pore characteristics and permeability[D]. Wuhan: Hubei University of Technology, 2015.

[16] WITT K J, BRAUNS J. Permeability-anisotropy due to particle shape[J]. Journal of Geotechnical Engineering, 1983, 109(9): 1181–1187.

[17] CHAPUIS R P, GILL D E. Hydraulic anisotropy of homogeneous soils and rocks: influence of the densification process[J]. Bulletin of the International Association of Engineering Geology, 198939: 75–86.

[18] ADAMS A L, GERMAINE J T, FLEMINGS P B, et al. Stress induced permeability anisotropy of Resedimented Boston Blue Clay[J]. Water Resources Research, 2013, 49(10): 6561–6571.

[19] LOUIS C. Rock hydraulics[J]. International Journal of Rock Mechanics and Mining Science & Geomechanics Abstracts, 1974, 12(4): 59.

[20] POTTS D M, ZDRAVKOVIC L. Finite element analysis in geotechnical engineering: application[M]. London: Thomas Telford, 2001: 35–72.

[21] WANG Chun-bo, DING Wen-qi, LIU Shu-bin, et al. Analysis of dynamic changes of anisotropic permeability coefficient with volumetric strain in seepage coupling[J]. Chinese Journal of Rock Mechanics and Engineering, 2014, 33(Suppl.1): 3015–3021.

[22] KONG Ling-rong. Study on pore distribution and permeability under different vertical stress levels due to consolidation of soft clay[J] Chinese Journal of Underground Space and Engineering, 2011, 7(Suppl.2): 1664–1666.

[23] YU Liang-gui. Experimental study on the effect of sedimentary environment and dynamic characteristics on permeability coefficient of soft clay[D]. Hangzhou: Zhejiang University, 2018.

[24] HORPIBULSUK S, YANGSUKKASEAM N, CHINKU-LKIJNIWAT A, et al. Compressibility and permeability of Bangkok clay compared with kaolinite and bentonite[J]. Applied Clay Science, 2011, 52(1–2): 150–159.

[25] CAO Yang. Experimental study on relationship between dynamic characteristics and microstructure of undisturbed soft clay under wave action[D]. Hangzhou: Zhejiang University, 2013.

[26] ZHAO Tie-jun, JIANG Fu-xiang. Submarine tunnel engineering durability technology[M]. Beijing: China Communications Press, 2010.

[27] LAPIERRE C, LEROUEIL S, LOCAT J. Mercury intrusion and permeability of Louiseville clay[J]. Canadian Geotechnical Journal, 1990, 27(6): 761–773.

[28] WANG Xiu-yan, LIU Chang-li. Discussion on permeability of deep clayey soil[J]. Chinese Journal of Geotechnical Engineering, 2003(3): 308–312.

[29] HORPIBULSUK S, YANGSUKKASEAM N, CHINKU-LKIJNIWAT A, et al. Compressibility and permeability of Bangkok clay compared with kaolinite and bentonite[J]. Applied Clay Science, 2011, 52(1–2): 150–159.

[30] JI Li-ming, QIU Jun-li, XIA Yan-qing, et al. Micro-pore characteristics and methane absorption properties of common clay minerals by electron microscope scanning[J]. Acta Petrolei Sinica, 2012, 33(2): 249–256.

[31] CUI De-shan, XIANG Wei, CAO Li-jing, et al. Experimental study on reducing thickness of adsorbed water layer for red clay particles treated by ionic soil stabilizer[J]. Chinese Journal of Geotechnical Engineering, 2010, 32(6): 944–949.